RSC Advances




ROYAL SOCIETY OF CHEMISTRY

www.rsc.org/advances

# Comparison of hyper-cross-linked polystyrene/polyacryldiethylenetriamine (HCP/PADETA) interpenetrating polymer networks (IPNs) with hyper-cross-linked polystyrene (HCP): Structure, adsorption and separation properties

Zhenyu Fu, Shan Han, Jianhan Huang*, You-Nian Liu*

*College of Chemistry and Chemical Engineering, Central South University, Changsha, Hunan 410083, China*

* Corresponding Authors. Tel./fax: +86-731-88879616. E-mail: jianhanhuang@csu.edu.cn (Jianhan Huang); liuyounian@csu.edu.cn (You-Nian Liu).

**Abstract:** A novel hyper-cross-linked polystyrene/polyacryldiethylenetriamine (HCP/PADETA) interpenetrating polymer networks (IPNs) was prepared, characterized and evaluated for its adsorption and separation properties, using hyper-cross-linked polystyrene (HCP) as the reference. In spite of its much less Brunauer-Emmett-Teller surface area and pore volume, HCP/PADETA IPNs possessed preferable pore structure and quite appropriate polarity, inducing its larger equilibrium capacity, faster adsorption rate, higher dynamic breakthrough and saturated capacity towards salicylic acid than HCP. In particular, HCP/PADETA IPNs had a high enrichment factor for salicylic acid over phenol, leading to its high-efficiency separation of salicylic acid from phenol in their mixed solution.

*Keywords:* Interpenetrating polymer networks (IPNs); Hyper-cross-linked polystyrene (HCP); Hyper-cross-linking; Adsorption; Salicylic acid

## 1. Introduction

In 1969, Davankov proposed a novel approach for producing a novel polymer named "hyper-cross-linked polystyrene (HCP)" [1]. HCP is recognized by its high Brunauer-Emmett-Teller (BET) surface area, predominant micro/mesopores and unprecedented adsorption property, and hence is considered as the most efficient polymeric adsorbent for adsorptive removal of non-polar and weakly polar aromatic compounds [2, 3]. HCP has also attracted many attentions as an excellent adsorbing material for high-performance liquid chromatography (HPLC), size-exclusion chromatography and solid-phase extraction [4-7]. HCP is frequently synthesized from linear polystyrene (PS) or low cross-linked poly(styrene-co-divinylbenzene) using monochloromethylether (MCME), *p*-dibenzenylchloride (DBC) or *p*-dichloromethylbenzene (DCMB) as the post-cross-linking reagent, the used reaction is the typical Friedel-Crafts reaction, and the Friedel-Crafts catalysts include anhydrous zinc chloride, iron (III) chloride and stannic (IV) chloride [1, 3]. In addition, it can also be prepared from macroporous low cross-linked chloromethylated polystyrene (CMPS) by consuming its own benzyl chloride on the surface [8-10].

Due to its hydrophobic surface, HCP possessed a low adsorption towards polar aromatic compounds [11]. In order to improve the surface hydrophlicity and increase the adsorption capacity of HCP towards polar aromatic compounds, it is usually modified by introducing polar monomers into the copolymers, using polar compounds as the cross-linking reagent and adding polar compounds in the Friedel-Crafts reaction [2, 9]. On the other hand, due to the randomness of the Friedel-Crafts reaction, an excessive cross-linking for the benzyl chloride of CMPS is inevitable at the beginning of the reaction, the cross-linking bridges created at the initial stage of the reaction are much more rigid than those formed later, and hence the pore structure of HCP is not uniform. The formed rigid region is named as "the magic area" [12, 13]. The magic area of HCP is significant for adsorption, storage and separation of gases such

as $N_2$, $H_2$, $CO_2$ and $CH_4$ [14, 15], while it is useless for adsorption of aromatic compounds because the limitation of molecular size of aromatic compounds make it difficult to diffuse into the narrow pores of HCP [12, 16, 17]. Avoiding the excessive cross-linking for the benzyl chloride of CMPS during the Friedel-Crafts reaction, which may lead to the improvement of pore structure of HCP and the adsorption capacity towards aromatic compounds.

We propose that the excessive cross-linking for the benzyl chloride of CMPS will be relieved as inserting another polymer networks in the pores of CMPS via a typical interpenetrating polymer networks (IPNs) technology. The introduced polymer networks in the IPNs will separate the benzyl chloride of CMPS effectively, leading to a preferable pore structure over HCP after the Friedel-Craft reaction. Therefore, the preferable pore structure of the modified HCP will bring a favorable adsorption performance towards aromatic compounds. In particular, in this study, we focused on improving the pore structure of HCP, and used the obtained novel HCP for adsorption and separation of salicylic acid from aqueous solution. For this purpose, methylacrylate (MA) was in situ polymerized in the pores of CMPS under the help of the initiator, and chloromethylated polystyrene/poly(methylacrylate) (CMPS/PMA) IPNs was prepared by a typical IPNs technology. The Friedel-Crafts reaction was then employed for CMPS networks of the IPNs, followed by an amination reaction for the PMA networks, and hence a novel hyper-cross-linked polystyrene/polyacryldiethylenetriamine (HCP/PADETA) IPNs was synthesized accordingly. After characterization of HCP/PADETA IPNs, the adsorption and separation performance of the novel hyper-cross-linked IPNs was investigated from aqueous solution in detail using salicylic acid and phenol as the adsorbates.

## 2. Materials and methods

### *2.1. Materials*

CMPS was purchased from Langfang Chemical Co. Ltd. (Hebei province, China), its cross-linking degree was 6%, chlorine content was 17.3% (w/w), BET surface area was 13.1

$m^2/g$, and average pore size was 25.2 nm. Methyl acrylate (MA) was supplied by Gray West Chengdu Chemical Co. Ltd. (Sichuan Province, China), and washed by 5% of NaOH (w/v), followed by de-ionized water, and then dried by anhydrous magnesium sulfate before use. Benzoyl peroxide (BPO) was obtained from Fuchen Chemical Reagents Factory (Tianjin, China), and methanol was used as the solvent to recrystallize BPO. Butyl acetate, triallylisocyanurate (TAIC), *n*-heptane, 1, 2-dichloroethane (DCE), anhydrous ferric (III) chloride and diethylenetriamine (DETA) were analytical reagents purchased from Yongda Chemical Company (Shandong province, China), and they are used without further purification. Salicylic acid and phenol employed as the adsorbates were analytical reagents obtained from Xiya reagent Chemical Company (Sichuan province, China) and used without further purification.

*2.2. Preparation of HCP/PADETA IPNs*

As shown in Scheme 1, three continuous processes, interpenetration, Friedel-Crafts reaction and amination reaction, were applied for HCP/PADETA IPNs. According to the sequential interpenetration method in Refs. [18, 19], 20 g CMPS was firstly swollen by a mixture of MA, TAIC, butyl acetate, *n*-heptane and BPO for 12 h. 18 g MA was used as the monomer and 2 g TAIC was applied as the cross-linking reagent. Butyl acetate and *n*-heptane were used as the porogens and they were 250% relative to CMPS (w/w), and the mass ratio of butyl acetate to *n*-heptane was set to be 4:1. The swollen CMPS was then filtered and added into 200 mL 0.05% of polyvinyl alcohol (PVA) aqueous solution (w/v). At a moderate stirring speed, the temperature of the mixture rose to 358 K and kept at this temperature for 12 h. MA was in situ polymerized in the pores of CMPS, and hence CMPS/PMA IPNs was prepared. CMPS/PMA IPNs was further cross-linked by the Friedel-Crafts reaction in Refs. [8, 9], which was the same as the synthetic procedure for HCP from CMPS. The first CMPS networks of the IPNs were post-cross-linked and HCP/PMA IPNs was achieved accordingly. Thereafter,

HCP/PMA IPNs was aminated by superfluous DETA at 393 K for 12 h, and the second PMA networks of the IPNs were chemically modified by amide and amino groups on the surface and HCP/PADETA IPNs was synthesized accordingly.

*(Scheme 1 can be inserted here)*

*2.3. Characterization*

Fourier transform infrared spectroscopy (FT-IR) of the IPNs was recorded on a Nicolet 510P Fourier transform infrared instrument in 500-4000 $cm^{-1}$ with a resolution of 1.0 $cm^{-1}$. The chlorine content of the IPNs was measured by the Volhard method in Ref. [20] and the weak basic exchange capacity of the IPNs was determined according to Ref. [21]. Surface morphologies of the IPNs were observed with a scanning electron microscopy (SEM, FEI Nova Nano SEM 230, 10 kV). The pore structure parameters of the IPNs were determined by $N_2$ adsorption isotherms at 77 K using a Micromeritics Tristar 3000 surface area and porosity analyzer, and the BET surface area, t-Plot surface area, pore volume, t-Plot pore volume and pore size distribution were obtained. The BET surface area and pore volume were calculated according to the BET model while the t-Plot surface area, t-Plot pore volume and the pore size distribution were calculated by applying the Barrett-Joyner-Halenda (BJH) method to the $N_2$ desorption data.

*2.4. Adsorption and separation experiments*

For the equilibrium adsorption, about 0.1 g of the IPNs was mixed with 50 mL of a series of salicylic acid aqueous solution with the concentration of about 200, 400, 600, 800 and 1000 mg/L (w/v). The series of mixture were shaken in a thermostatic oscillator at a desired temperature (298, 308 or 318 K) until the equilibrium was reached. The absorbency of salicylic acid was analyzed via a Shimadzu UV-2450 spectrophotometer at a wavelength of 296.5 nm, and the equilibrium adsorption capacity of salicylic acid on the IPNs, $q_e$ (mg/g), was calculated based on the following equation:

$$q_e = (C_0 - C_e) \cdot V / W \qquad (Eq.1)$$

where $C_0$ is the initial concentration of salicylic acid (mg/L), $C_e$ is the equilibrium concentration of salicylic acid (mg/L), $V$ is the volume of the solution (L) and $W$ is the mass of the IPNs (g). The equilibrium adsorption capacity of phenol on the IPNs was determined via an UV-2450 spectrophotometer at a wavelength of 269.0 nm by the similar method for salicylic acid.

For the kinetic adsorption, about 1.0 g of the IPNs was mixed with 250 mL of salicylic acid solution at the initial concentration of 604.3, 804.3 or 1003.8 mg/L, respectively. The flasks were then continuously shaken until the adsorption equilibrium was reached. In this process, 0.50 mL of the solution was withdrawn at a set interval and the concentration of salicylic acid was determined, the adsorption capacity at a contact time $t$ was calculated as:

$$q_t = (C_0 - C_t) \cdot V / W \qquad (Eq.2)$$

where $q_t$ (mg/g) and $C_t$ represent the adsorption capacity and the concentration at contact time $t$ (mg/L), respectively.

For the column adsorption and desorption, 10 mL of the wetted IPNs was densely packed in a glass column with an inner size of 16 mm, salicylic acid aqueous solution at an initial concentration of 1017.3 mg/L was passed through the resin column at a flow rate of 1.0 mL/min, the concentration of salicylic acid in the effluent from the column exit, $C$ (mg/L), was continuously recorded until it nearly reached the initial concentration. After the column adsorption, the given desorption solvent passed through the resin column at a flow rate of 0.6 mL/min, the concentration of salicylic acid in the effluent was determined until it was close to zero.

For the dynamic separation experiment, a mixed solution containing 513.1 mg/L of salicylic acid and 489.5 mg/L of phenol was passed through the wetted IPNs (10 mL) at a flow rate of 1.5 mL/min, and the concentration of salicylic acid as well as phenol in the effluent from the column exit was continuously recorded until it nearly reached the initial concentration.

The desorption solvent was used for the desorption of the IPNs and the concentration of salicylic acid as well as phenol was determined.

## 3. Results and discussion

### *3.1. Characterization*

After interpenetration of PMA in the pores of CMPS, two strong vibrations at 1736 and 1701 $cm^{-1}$ [22-24] presented in the FT-IR spectrum of CMPS/PMA IPNs (Fig. 1), these two peaks are the C=O stretching of the ester carbonyl groups of MA and the amide carbonyl groups of TAIC, respectively. After the Friedel-Crafts reaction, the chlorine content decreased to 3.2%, two strong vibrations of the $-CH_2Cl$ groups at 1263 and 675 $cm^{-1}$ were greatly weakened, while other vibrations were similar with HCP. Li et al [25], Pan et al [26] and Huang et al [27, 28] got the similar results. After the amination, the vibration at 1736 $cm^{-1}$ was sharply reduced, while a new strong band appeared at 1650 $cm^{-1}$, and this band is concerned with C=O stretching of the amide carbonyl groups [29]. In particular, the weak basic exchange capacity of HCP/PADETA IPNs was 2.107 mmol/g. All of these results suggested that the interpenetration, Friedel-Crafts reaction and amination reaction were carried out successfully and HCP/PADETA IPNs was synthesized accordantly. Fig. S1 shows the SEM images of CMPS, CMPS/PMA IPNs, HCP/PMA IPNs and HCP/PADETA IPNs, respectively. It is interesting to observe that the surface of CMPS/PMA IPNs and HCP/PMA IPNs is much smoother than that of the CMPS, while the surface of HCP/PADETA IPNs is rougher than that of HCP/PMA IPNs, which is in accord with the reaction processes.

*(Fig. 1 can be inserted here)*

The BET surface area and pore volume decreased after interpenetration of PMA in the pores of CMPS (Table 1), while they increased significantly after the Friedel-Crafts reaction, Ahn et al [7], Fontanals et al [30] and Urban et al [31] reported the similar results. Additionally, the BET surface area and pore volume of HCP/PMA IPNs were much less than those of HCP,

implying that the introduced PMA networks separated the benzyl chloride of CMPS networks successfully and the excessive cross-linking of CMPS was controlled effectively. Specifically, 240.3 $m^2/g$ of t-plot micropore surface area and 0.3350 $cm^3/g$ of t-plot micropore volume were measured for HCP/PMA IPNs, while that of HCP were predicted to be 570.9 $m^2/g$ and 0.5980 $cm^3/g$, respectively. In addition, the amination reaction decreased the BET surface area and pore volume, which may be from the increased polarity [9, 19, 26].

*(Table 1 can be inserted here)*

Fig. 2 (a) indicates that the macropores are the dominant pores for CMPS and CMPS/PMA IPNs, whereas mesopores ranging from 2 to 5 nm are predominant for HCP/PMA IPNs and HCP/PADETA IPNs. Actually, the average pore size of CMPS/PMA IPNs is 9.52 nm, while that of HCP/PADETA IPNs is 2.77 nm, confirming that plenty of micropores are produced. As compared the pore size distribution of HCP/PADETA IPNs with HCP (Fig. 2 (b)), it is interesting to observe that HCP/PADETA IPNs owns a much less pore volume while has a peak in 4 nm, and its average pore size is a bit bigger than HCP (2.45 nm), which states that the introduced PMA networks partially control the excessive cross-linking of CMPS in Friedel-Crafts reaction and the pore structure of HCP/PADETA IPNs is better than HCP.

*(Fig. 2 can be inserted here)*

*3.2. Equilibrium adsorption*

The equilibrium adsorption of CMPS, CMPS/PMA IPNs, HCP/PMA IPNs and HCP/PADETA IPNs were comparatively studied using salicylic acid as the adsorbate and the results are displayed in Fig. 3 (a). The adsorption of CMPS and CMPS/PMA IPNs is very weak, which may be attributed to their low BET surface area. After the Friedel-Crafts reaction, HCP/PMA IPNs has a much larger equilibrium capacity, which may be partly due to the sharply increased BET surface area and the predominant mico/mesopores [5, 32]. What's more, HCP/PMADETA IPNs showed an enhanced adsorption in comparison with HCP/PMA IPNs in

spite of its decreased BET surface area and pore volume. The uploaded amide and amino groups on the surface should contribute to the increased adsorption [28, 32].

*(Fig. 3 can be inserted here)*

In addition, Fig. 3 (b) indicates that HCP/PADETA IPNs is superior to HCP as considering the adsorption of salicylic acid. Even though the BET surface area of HCP/PADETA IPNs is lower by up to 65.1% than HCP, the pore structure of HCP/PADETA IPNs is better than HCP. What's more, the uploaded amide and amino groups on the surface of HCP/PADETA IPNs may make the adsorption performance enhanced due to the polarity matching, and there may exist possible hydrogen bonding between the amide and amino groups of HCP/PADETA IPNs and the phenolic hydroxyl, carboxyl groups of salicylic acid.

At an equilibrium concentration of 100 mg/L, HCP/PADETA IPNs possesses an equilibrium capacity of 313.3 mg/g, which is 87.8 times higher than CMPS, 143.4 times higher than CMPS/PMA IPNs, 4.5 times higher than HCP/PMA IPNs and 1.6 times higher than HCP, respectively. As compared with some other materials, HCP/PADETA IPNs is shown to be superior to the results reported in Ref. [33] (43.0 mg/g by Duolite S861; 85.1 mg/g by Amberlite XAD16), Ref. [34] (70.0 mg/g by XAD-4; 125.0 mg/g by an amino modified hyper-cross-linked resin), Ref. [9] (205.0 mg/g by an amide-modified hyper-cross-linked resin) and this work (195.6 mg/g by HCP).

Additionally, the equilibrium isotherms in Fig. S2 shows that the equilibrium capacity increases with increasing of the temperature, demonstrating that the interaction between HCP/PADETA IPNs and salicylic acid is strengthened at a higher temperature and the adsorption is an endothermic process [35]. Langmuir and Freundlich models were used to describe the equilibrium process [36, 37] and the corresponding parameters such as $q_m$, $K_L$, $K_F$ and $n$ as well as the correlation coefficients $R^2$ were summarized in Table S1. Both of the Langmuir and Freundlich models appears to be appropriate for fitting the equilibrium data due

to the high correlative coefficients ($R^2$>0.98), the *n* values of the Freundlich model for the adsorption are greater than 1, implying that the adsorption is a very favorable process. In particular, only the Freundlich model can fit the equilibrium data on HCP, which is different from the adsorption performance of HCP/PADETA IPNs.

*3.3. Kinetic adsorption*

The kinetic curves of salicylic acid adsorption on HCP/PADETA IPNs and HCP were comparatively measured and the results are illustrated in Fig. 4. It is obvious that the adsorption capacity increases rapidly with increasing of the adsorption time, and the adsorption capacity reaches over 75% of the equilibrium capacity within one hour, suggesting that the adsorption is a fast process. Moreover, HCP/PADETA IPNs is more efficient than HCP and it needs much less time to reach equilibrium than HCP. The adsorption capacity reaches 96% of the equilibrium capacity within one hour for HCP/PADETA IPNs, while only 75% is arrived for HCP, which further confirms that HCP/PADETA IPNs has a more favorable pore structure for diffusion of salicylic acid in the pores.

*(Fig. 4 can be inserted here)*

The pseudo-first-order rate equation and the pseudo-second-order equation [38, 39] were employed for characterizing the kinetic data and the corresponding parameters are summarized in Table 2. Both of the pseudo-first-order and the pseudo-second-order rate equations are suitable for fitting the kinetic data on HCP/PADETA IPNs, and the predicted equilibrium capacity is much larger than HCP. Additionally, the values of $k_2$ on HCP/PADETA IPNs and HCP were predicted to be $1.29\times10^{-3}$ and $3.10\times10^{-4}$ g/(mg·min), respectively, agreeing with the fact that the adsorption rate on HCP/PADETA IPNs is much faster than HCP.

*(Table 2 can be inserted here)*

Additionally, the kinetic curves for the adsorption of salicylic acid on HCP/PADETA IPNs with the initial concentration of 604.3, 804.3 and 1003.8 mg/L and the temperature at 293, 303

and 313 K are measured (Fig. S3). At a higher temperature, less time is required to reach equilibrium, implying that the adsorption rate is faster at a higher temperature, while more time is needed to reach equilibrium at a higher initial concentration, which may be from the increased collision of salicylic acid in the solution. The pseudo-first-order and pseudo-second-order rate equations were applied for simulation of the kinetic data and the corresponding parameters are listed in Table S2. Both of the pseudo-first-order and pseudo-second-order rate equations are suitable for characterizing the kinetic data. The values of $k_2$ at 293, 303 and 313 K are predicted to be $1.29\times10^{-3}$, $1.37\times10^{-3}$ and $1.84\times10^{-3}$ g/(mg·min), respectively, which is accordant with the fact that the adsorption rate is faster at a higher temperature.

*3.4. Column adsorption and desorption*

Fig. 5 shows the column adsorption and desorption properties of salicylic acid on HCP/PADETA IPNs and HCP, the shape of the dynamic adsorption curve is very sharp, meaning that the adsorption reaches equilibrium quickly after leakage [40]. We defined $C/C_0$=0.05 (where $C$ is the concentration of salicylic acid from the effluent, mg/L) as the breakthrough point and $C/C_0$=0.95 as the saturated point, and the volume of the effluent to reach the breakthrough point and the saturated point was defined as $V_b$ and $V_s$, respectively. Fig. 5 (a) indicates that $V_b$ is 109.1 BV (1 BV=10 mL) and $V_s$ is 163.3 BV for HCP/PADETA IPNs, much greater than HCP (81.4 and 116.6 BV, respectively). The dynamic saturated capacities were 137.6 and 92.6 mg/mL wet resins for HCP/PADETA IPNs and HCP, respectively.

*(Fig. 5 can be inserted here)*

After the column adsorption, different desorption solvents were employed for the desorption process (Fig. S4). 0.01 mol/L of NaOH (w/v) and 20% of ethanol (v/v) are proven the best desorption solvent for desorption of the resin column. It was utilized for the column desorption and the results are dispalyed in Fig. 5 (b). At a flow rate of 0.6 mL/min, only 20 BV

of the desorption solvent is enough to completely regenerate the resin column, and the dynamic desorption capacity was 1320.0 and 858.6 mg for HCP/PADETA IPNs and HCP, respectively, which is coincident with the dynamic saturated capacity (1376.0 and 926.3 mg) in the column adsorption. Moreover, the desorption of HCP/PADETA IPNs is faster than HCP, and less desorption solvent is needed for the desorption, demonstrating that the pore structure of HCP/PADETA IPNs is superior to HCP. HCP/PADETA IPNs was used repeatedly for five cycles in a continuous adsorption-desorption process. In the first run, the recovery rate ( the ratio of desorption to adsorption) of salicylic acid is 97.6%, which means HCP/PADETA IPNs can be used as a good adsorbent to enrich salicylic acid. Moreover, the salicylic acid uptakes decreased to approximately 84.5% after five cycles of the adsorption-desorption process, exhibiting good reusability and regeneration behaviors (Fig. S5).

*3.5. Separation of salicylic acid from phenol in their mixed solution*

Salicylic acid is generally produced from phenol and hence phenol may jointly exist with salicylic acid [41]. Therefore, selective adsorption of salicylic acid on the adsorbent as well as separation of salicylic acid from phenol is of great importance [33]. As compared with phenol, salicylic acid has another carboxyl group, and the carboxyl group is at the *ortho*-position with respect to the phenolic hydroxyl group. Moreover, the neighboring carboxyl group can form intramolecular hydrogen bond with the phenolic hydroxyl group [42], which makes salicylic acid a well-balanced molecule with both of hydrophobic portion and hydrophilic portion. HCP/PADETA IPNs in this study possesses hydrophobic HCP networks as well as hydrophilic PADETA networks. Therefore, as can be seen from Fig. 3, HCP/PADETA IPNs achieves a highly efficient adsorption towards salicylic acid. The hydrophobic HCP networks have a relatively strong affinity to the hydrophobic portion of salicylic acid due to the hydrophobic interaction or π-π stacking, [43, 44], whereas the hydrophilic PADETA networks are more inclined to approach the hydrophilic portion of salicylic acid by the possible electrostatic

interaction or hydrogen bonding [22, 27, 40]. Nevertheless, some other molecules like phenol is not adsorbed effectively, and separation of salicylic acid from phenol is possible. For this reason, a mixed adsorption test was conducted for salicylic acid and phenol and the results are shown in Fig. 6. The enrichment factor was used as a performance parameter to evaluate adsorption [45]. The distribution ratio (*D*) is given by Eq. (3):

*(Fig. 6 can be inserted here)*

$$D = \frac{C_0 - C_e}{C_0} \times \frac{V}{M} \qquad \textit{(Eq. 3)}$$

where $C_0$ is the initial concentration of the adsorbate in solution, $C_e$ is the concentration of the adsorbate in the aqueous phase after adsorption, respectively (mg/L), $V$ is the volume of the aqueous phase (mL), and $M$ is the amount of HCP/PADETA IPNs (g).

The enrichment factor (α) for the adsorption of salicylic acid in the presence of phenol can be obtained from the equilibrium distribution ratio according to Eq. (4):

$$\alpha = \frac{D_{SA}}{D_{phenol}} \qquad \textit{(Eq. 4)}$$

where $D_{SA}$ and $D_{phenol}$ represent the distribution ratios of salicylic acid and phenol, respectively.

In the single solution, the equilibrium capacity of salicylic acid on HCP/PADETA IPNs was 313.3 mg/g at an equilibrium concentration of 100 mg/L, much larger than phenol (42.6 mg/g), and the enrichment factor is 10.3. The enrichment factor of HCP/PADETA IPNs is much higher than HCP. In the mixed solution, the equilibrium capacity of salicylic acid increased to 337.1 mg/g, while that of phenol decreased to 18.6 mg/g, and the enrichment factor (α) increased to 17.3, suggesting that the adsorption of salicylic acid and phenol is competitive, and the adsorption of salicylic acid from the mixed solution is enhanced. Hence, it is possible to separate of salicylic acid from phenol in their mixed solution by HCP/PADETA IPNs [46].

As shown in Fig 7. The $V_b$ was measured to be 255.0 BV for salicylic acid at a flow rate of 1.5 mL/min, much greater than phenol (30.0 BV). The corresponding saturated capacity for salicylic acid is 178.0 mg/mL wet resins, much greater than phenol (6.4 mg/mL wet resins). That is, only phenol is existent in the effluent ranging from 0 to 255 BV and the collected effluent is a pure phenol solution, whereas salicylic acid is concentrated on the resin column. In particular, in the range of 127-722 BV, the concentration of phenol is higher than its initial one ($C/C_0$>1.0), confirming that HCP/PADETA IPNs has a stronger affinity to salicylic acid than phenol, and the pre-loaded phenol molecules on the resin column are pushed out by the following salicylic acid molecules. The excluded amount of phenol from the resin column is 82.4% (w/w). After desorption of the resin column, both of phenol and salicylic acid are desorbed from the resin column, 2122 mg of salicylic acid and 60 mg of phenol are collected, and the concentration of salicylic acid increases from 50.1% to 97.2% (w/w).

*(Fig. 7 can be inserted here)*

## 4. Conclusions

HCP/PADETA IPNs was prepared from CMPS by interpenetration of PMA networks in the pores of CMPS, self cross-linked reaction of the benzyl chloride of CMPS networks and amination reaction of PMA networks with DETA, and its adsorption and separation properties were evaluated using HCP as the reference. The BET surface area HCP/PADETA IPNs was only 55% of HCP, while the introduced PMA networks separated the benzyl chloride of CMPS networks successfully and the excessive cross-linking of CMPS was controlled effectively, which induced to its preferable pore structure. HCP/PADETA possessed a very large equilibrium capacity towards salicylic acid, and it reached 313.3 mg/g at an equilibrium concentration of 100 mg/L, which was 1.6 times higher than HCP. HCP/PADETA IPNs was highly efficient for the adsorption of salicylic acid and required much less time to reach equilibrium than HCP. In addition, the dynamic saturated capacity of salicylic acid was 137.6

mg/mL wet resins for HCP/PADETA IPNs, much greater than HCP. Moreover, HCP/PADETA IPNs had an enrichment factor of 17.3 for salicylic acid over phenol, and it separated salicylic acid from phenol successfully in their mixed solution.

**Acknowledgments**

The authors thank the National Natural Science Foundation of China (No. 21376275), the Fundamental Research Funds for the Central Universities of Central South University (No. 2015zzts020) and South Wisdom Valley Innovative Research Team Program for the financial support. The authors also thank Prof. Kirin in Ruđer Bošković Institute of Croatia for his helpful suggestion.

**References**

[1] V.A. Davankov, M.P. Tsyurupa, Structure and properties of hypercrosslinked polystyrene-the first representative of a new class of polymer networks, *React. Polym.* 13 (1990) 27-42.

[2] C. Valderrama, X. Gamisans, F.X. De las Heras, J.L. Cortina, A. Farran, Kinetics of polycyclic aromatic hydrocarbons removal using hyper-cross-linked polymeric sorbents Macronet Hypersol MN200, *React. Funct. Polym.* 67 (2007) 1515-1529.

[3] M.P. Tsyurupa, V.A. Davankov, Porous structure of hypercrosslinked polystyrene: state-of-the-art mini-review, *React. Funct. Polym.* 66 (2006) 768-779.

[4] R. Frassanito, M. Rossi, L.K. Dragani, C. Tallarico, A. Longo, D. Rotilio, New and simple method for the analysis of the glutathione adduct of atrazine, *J. Chromatogr. A* 795 (1998) 53-60.

[5] J. Urban, F. Svec, J.M. Fréchet, Efficient separation of small molecules using a large surface area hypercrosslinked monolithic polymer capillary column, *Anal. Chem.* 82 (2010) 1621-1623.

[6] K. Jeřábek, M. Zecca, P. Centomo, F. Marchionda, L. Peruzzo, P. Canton, E. Negro, V.D.

Noto, B. Corain, Synthesis of nanocomposites from Pd and a hyper-cross-linked functional resin obtained from a conventional gel-type precursor. *Chem. Eur. J.* 19 (2013) 9381-9387.

[7] J.H. Ahn, J.E. Jang, C.G. Oh, S.K. Ihm, J. Cortez, D.C. Sherrington, Rapid generation and control of microporosity, bimodal pore size distribution, and surface area in Davankov-type hyper-cross-linked resins. *Macromolecules* 39 (2006) 627-632.

[8] X. Ling, H.B. Li, H.W. Zha, C.L. He, J.H. Huang, Polar-modified post-cross-linked polystyrene and its adsorption towards salicylic acid from aqueous solution, *Chem. Eng. J.* 286 (2016) 400-407.

[9] H.B. Li, Z.Y. Fu, C. Yan, J.H. Huang, Y.N. Liu, S.I. Kirin, Hydrophobic-hydrophilic post-cross-linked polystyrene/poly (methyl acryloyl diethylenetriamine) interpenetrating polymer networks and its adsorption properties, *J. Colloid Interf. Sci.* 63 (2016) 61-68.

[10] M. Seo, S. Kim, Oh, J. S.J. Kim, M.A. Hillmyer, Hierarchically porous polymers from hyper-cross-linked block polymer precursors, *J. Am. Chem. Soc.* 137 (2015) 600-603.

[11] C. Valderrama, J.L. Cortina, A. Farran, X. Gamisans, F.X. De Las Heras, Evaluation of hyper-cross-linked polymeric sorbents (Macronet MN200 and MN300) on dye (Acid red 14) removal process, *React. Funct. Polym.* 68 (2008) 679-691.

[12] C.D. Wood, B. Tan, A.Trewin, H. Niu, D. Bradshaw, M.J. Rosseinsky, Y.Z. Khimyak, N.L. Campbell, R. Kirk, E. Stöckel, Hydrogen storage in microporous hypercrosslinked organic polymer networks, *Chem. Mater*. 19 (2007) 2034-2048.

[13] M. Errahali, G. Gatti, L. Tei, G. Paul, G.A. Rolla, L. Canti, A. Fraccarollo, M. Cossi, A. Comotti, P. Sozzani, L. Marchese, Microporous hyper-cross-linked aromatic polymers designed for methane and carbon dioxide adsorption, *J. Phys. Chem. C* 118 (2014) 28699-28710.

[14] J.S. Zhang, Z.A. Qiao, S.M. Mahurin, X.G. Jiang, S.H. Chai, H.F. Lu, K. Nelson, S. Dai, Hypercrosslinked phenolic polymers with well-developed mesoporous frameworks,

*Angew. Chem. Int. Ed.* 54 (2015) 4582-4586.

[15] L. Pan, Q. Chen, J.H. Zhu, J.G. Yu, Y.J. He, B.H. Han, Hypercrosslinked porous polycarbazoles via one-step oxidative coupling reaction and Friedel-Crafts alkylation, *Polym. Chem.* 6 (2015) 2478-2487.

[16] N. Fontanals, J. Cortés, M. Galià, R.M. Marcé, P.A. Cormack, F. Borrull, D.C. Sherrington, Synthesis of Davankov-type hypercrosslinked resins using different isomer compositions of vinylbenzyl chloride monomer, and application in the solid-phase extraction of polar compounds, *J. Polym. Sci. Pol. Chem.* 43 (2005) 1718-1728.

[17] D. Bratkowska, N. Fontanals, F. Borrull, P.A.G. Cormack, D.C. Sherrington, R.M. Marcé, Hydrophilic hypercrosslinked polymeric sorbents for the solid-phase extraction of polar contaminants from water, *J. Chromatogr. A* 1217 (2010) 3238-3243.

[18] X.M. Wang, Z.Y. Fu, N. Yu, J.H. Huang, A novel polar-modified post-cross-linked resin: Effect of the porogens on the structure and adsorption performance, *J. Colloid Interf. Sci.* 466 (2016) 322-329.

[19] X.M. Wang, L.M. Chen, Y.N. Liu, J.H. Huang, Macroporous crosslinked polydivinylbenzene/polyacryldiethylenetriamine (PDVB/PADETA) interpenetrating polymer networks (IPNs) and their efficient adsorption to *o*-aminobenzoic acid from aqueous solution, *J. Colloid Interf. Sci.* 429 (2014) 83-87.

[20] C.P. Wu, C.H. Zhou, F.X. Li. *Experiments of Polymeric Chemistry*, Anhui Science and Technology Press, Hefei, 1987.

[21] B.L. He, W.Q. Huang. *Ion Exchange and Adsorption Resin*, Shanghai Science and Technology Education Press, Shanghai, 1995.

[22] X.M. Wang, P.D Patil, C.L. He, J.H. Huang, Y.N. Liu, Acetamide-modified hyper-cross-linked resin: Synthesis, characterization and adsorption performance to phenol from aqueous solution, *J. Appl. Polym. Sci.* 132 (2015) 41597 (1-9).

[23] Z.Y. Fu, H.B. Li, L. Yang, H. Yuan, Z.H. Jiao, L.M. Chen, J.H. Huang, Y.N. Liu, Magnetic polar post-cross-linked resin and its adsorption towards salicylic acid from aqueous solution, *Chem. Eng. J.* 273 (2015) 240-246.

[24] H.B. Li, Z.Y. Fu, L. Yang, C. Yan, L.M. Chen, J.H. Huang, Y.N. Liu, Synthesis and adsorption property of hydrophilic-hydrophobic macroporous crosslinked poly(methyl acryloyl diethylenetriamine)/poly(divinylbenzene)(PMADETA/PDVB) interpenetrating polymer networks (IPNs), *RSC Adv.* 5 (2015) 26616-26624.

[25] G.Q. Xiao, L.C. Fu, A.M. Li, Enhanced adsorption of bisphenol A from water by acetylaniline modified hyper-cross-linked polymeric adsorbent: Effect of the cross-linked bridge, *Chem. Eng. J.* 191 (2012) 171-176.

[26] B.C Pan, Q.J. Zhang, W. Du, B.J. Pan, W.M. Zhang, Q.R. Zhang, Q.X Zhang, Removal of aromatic sulfonates from aqueous media by aminated polymeric sorbents: Concentration-dependent selectivity and the application, Micropor. Mesopor. Mater. 116 (2008) 63-69.

[27] X.M. Wang, Q.L. Zeng, J.H. Huang, Y.N. Liu, A β-naphthol-modified hyper-cross-linked resin for adsorption of *p*-aminobenzoic acid from aqueous solutions, *Desalin. Water Treat.* 54 (2015) 1893-1902.

[28] Z.Y. Fu, C.L. He, J.H. Huang, Y.N. Liu, Polar modified post-cross-linked resin and its adsorption toward salicylic acid from aqueous solution: Equilibrium, kinetics and breakthrough studies, *J. Colloid. Interf. Sci.* 451 (2015) 1-6.

[29] B.H. Stuart, *Infrared Spectroscopy: Fundamentals and Applications*, John Wiley & Sons, 2004.

[30] N. Fontanals, P. Manesiotis, D.C. Sherrington, P.A. Cormack, Synthesis of spherical ultra-high-surface-area monodisperse amphipathic polymer sponges in the low-micrometer size range, *Adv. Mater.* 20 (2008) 1298-1302.

[31] J. Urban, F. Svec, J.M. Fréchet, Hypercrosslinking: new approach to porous polymer monolithic capillary columns with large surface area for the highly efficient separation of small molecules, *J. Chromatogr. A* 1217 (2010) 8212-8221.

[32] X.F. Jiang, J.H. Huang, Adsorption of Rhodamine B on two novel polar-modified post-cross-linked resins: Equilibrium and kinetics, *J. Colloid Interf. Sci.* 467 (2016) 230-238.

[33] M. Otero, M. Zabkova, A.E. Rodrigues, Comparative study of the adsorption of phenol and salicylic acid from aqueous solution onto nonionic polymeric resins, *Sep. Purif. Technol.* 45 (2005) 86-95.

[34] G.Q. Xiao, H. Li, M.C. Xu, Adsorption of salicylic acid in aqueous solution by a water-compatible hyper-cross-linked resin functionalized with amino-group, *J. Appl. Polym. Sci.* 127 (2013) 3858-3863.

[35] D.D. Do, *Adsorption analysis*, World Scientific, 1998.

[36] I. Langmuir, the constitution and fundamental properties of solids and liquids, Part I. solids, *J. Am. Chem. Soc.* 38 (1916) 2221-2295.

[37] H.M.F. Freundlich, Over the adsorption in solution, *J. Phys. Chem.* 57 (1906) 1100-1107.

[38] S. Lagergren, About the theory of so-called adsorption of soluble substances, *Kungliga Svenska Vetenskapsakademiens Handlingar*, 24 (1898) 1-39.

[39] Y.S. Ho, G. McKay, Sorption of copper (II) from aqueous solution by peat, *Water, Air, Soil Pollut.* 158 (2004) 77-97.

[40] Z.Y. Fu, C.L. He, H.B. Li, C. Yan, L.M. Chen, J.H. Huang, Y.N. Liu, A novel hydrophilic-hydrophobic magnetic interpenetrating polymer networks (IPNs) and its adsorption towards salicylic acid from aqueous solution, *Chem. Eng. J.* 279 (2015) 250-257.

[41] M. Otero, C.A. Grande, A.E. Rodrigues, Adsorption of salicylic acid onto polymeric

adsorbents and activated charcoal, *React. Funct. Polym.* 60 (2004) 203-213.

[42] Q.W. Wang, Y.H. Yang, H.B. Gao, *Hydrogen Bonding in Organic chemistry*, Tianjin: Tianjin University Press, 1983.

[43] Y.Q. Hu, T. Guo, X.S. Ye, Q. Li, M. Guo, H.N. Liu, Z.J. Wu, Dye adsorption by resins: Effect of ionic strength on hydrophobic and electrostatic interactions, *Chem. Eng. J.* 228 (2013) 392-397.

[44] C.G. Perkins, J.E. Warren, A. Fateeva, K.C. Stylianou, A. McLennan, K. Jelfs, D. Bradshaw, M.J. Rosseinsky, A porous layered metal-organic framework from π-π-stacking of layers based on a $Co_6$ building unit, *Micropor. Mesopor. Mater.* 157 (2012) 24-32.

[45] Y. Jiang, D. Kim. Effect of solvent/monomer feed ratio on the structure and adsorption properties of $Cu^{2+}$-imprinted microporous polymer particles, *Chem. Eng. J.* 166 (2011) 435-444.

[46] M. Moeder. *Phenols analysis in environmental samples*, John Wiley & Sons, Ltd, 2000.

Table 1 Structural parameters of CMPS, CMPS/PMA IPNs, HCP/PMA IPNs, HCP/PADETA IPNs and HCP, respectively.

| | CMPS | CMPS/PMA IPNs | HCP/PMA IPNs | HCP/PADETA IPNs | HCP |
|---|---|---|---|---|---|
| BET surface area /($m^2$/g) | 13.1 | 3.4 | 521.6 | 330.7 | 948.2 |
| t-Plot micropore surface area /($m^2$/g) | - | - | 240.3 | 150.3 | 570.9 |
| Pore volume /($cm^3$/g) | 0.0240 | 0.0080 | 0.3350 | 0.2030 | 0.5980 |
| t-Plot micropore volume /($cm^3$/g) | - | - | 0.154 | 0.117 | 0.336 |
| Average pore size /(nm) | 7.43 | 9.52 | 2.68 | 2.77 | 2.45 |

Table 2 Correlative parameters of kinetic data of salicylic acid on HCP and HCP/PADETA IPNs according to the pseudo-first-order and pseudo-second-order rate equations.

| | Pseudo-first-order rate | | | Pseudo-second-order rate | | |
|---|---|---|---|---|---|---|
| | $k_1$ ($min^{-1}$) | $q_e$(mg/g) | $R^2$ | $k_2$(g/(mg·min)) | $q_e$(mg/g) | $R^2$ |
| HCP | 0.0299 | 116.8 | 0.9678 | 0.00031 | 130.8 | 0.9926 |
| HCP/PADETA IPNs | 0.1342 | 142.3 | 0.9899 | 0.00129 | 155.0 | 0.9961 |

Scheme 1 The synthetic procedure of HCP/PADETA IPNs

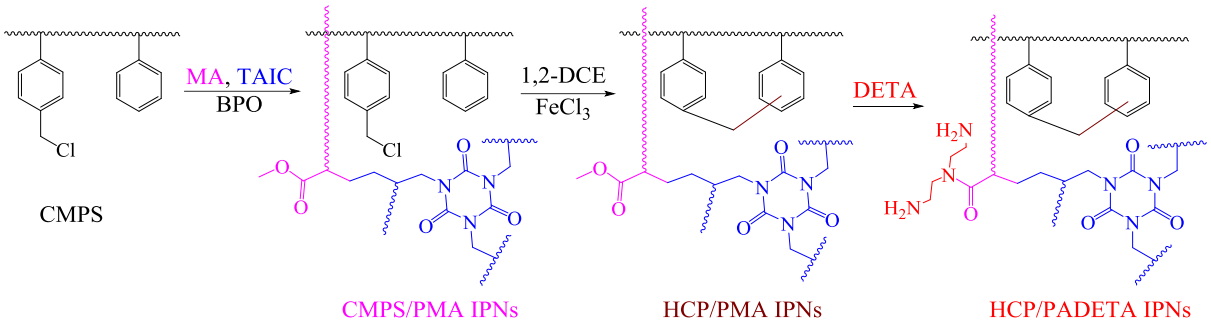

Fig. 1 FT-IR spectra of CMPS, CMPS/PMA IPNs, HCP/PMA IPNs, HCP/PADETA IPNs and HCP, respectively.

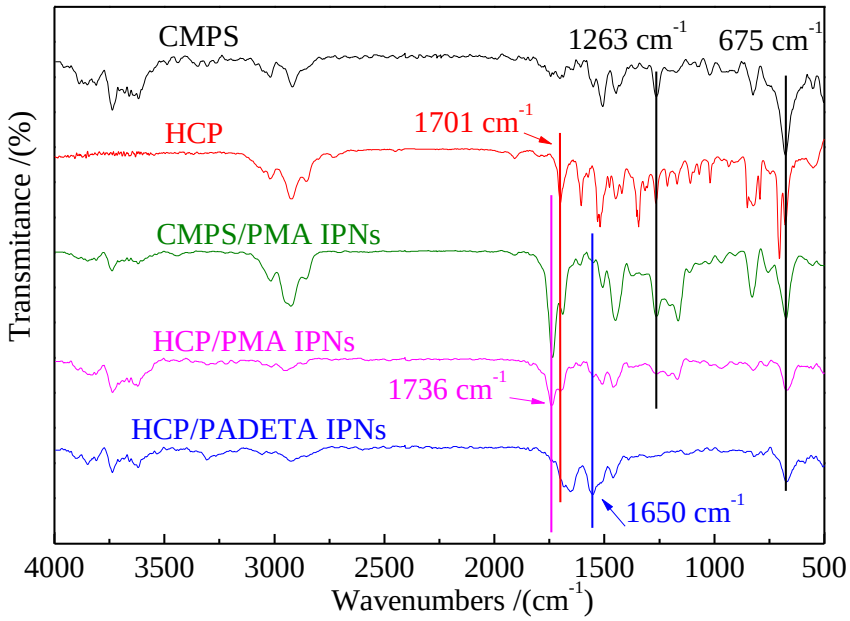

Fig. 2 Pore size distribution of (a) CMPS, CMPS/PMA IPNs, HCP/PMA IPNs and HCP/PADETA IPNs, (b) HCP and HCP/PADETA IPNs.

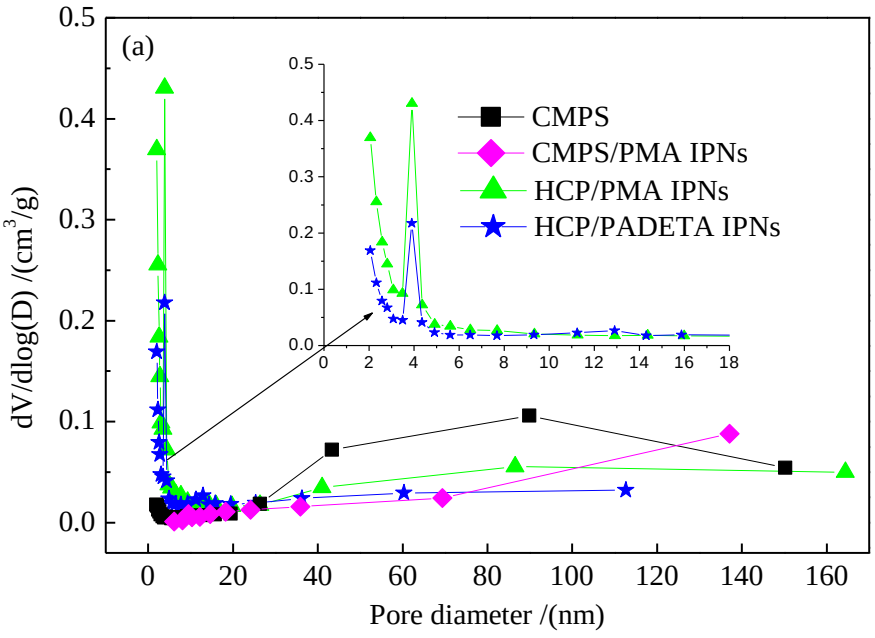


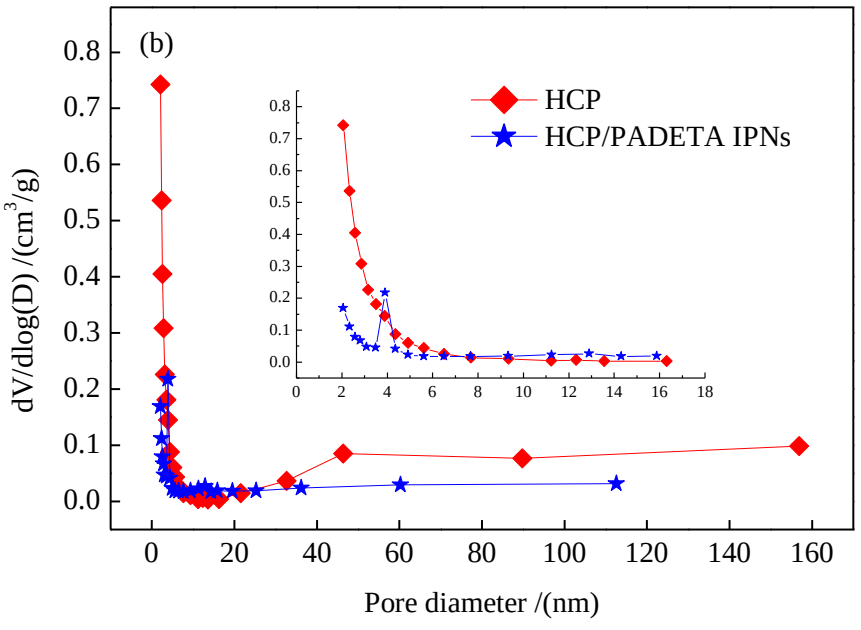

Fig. 3 Equilibrium isotherms of salicylic acid on (a) CMPS, CMPS/PMA IPNs, HCP/PMA IPNs and HCP/PADETA IPNs; (b) HCP and HCP/PADETA IPNs from aqueous solution at 298 K.

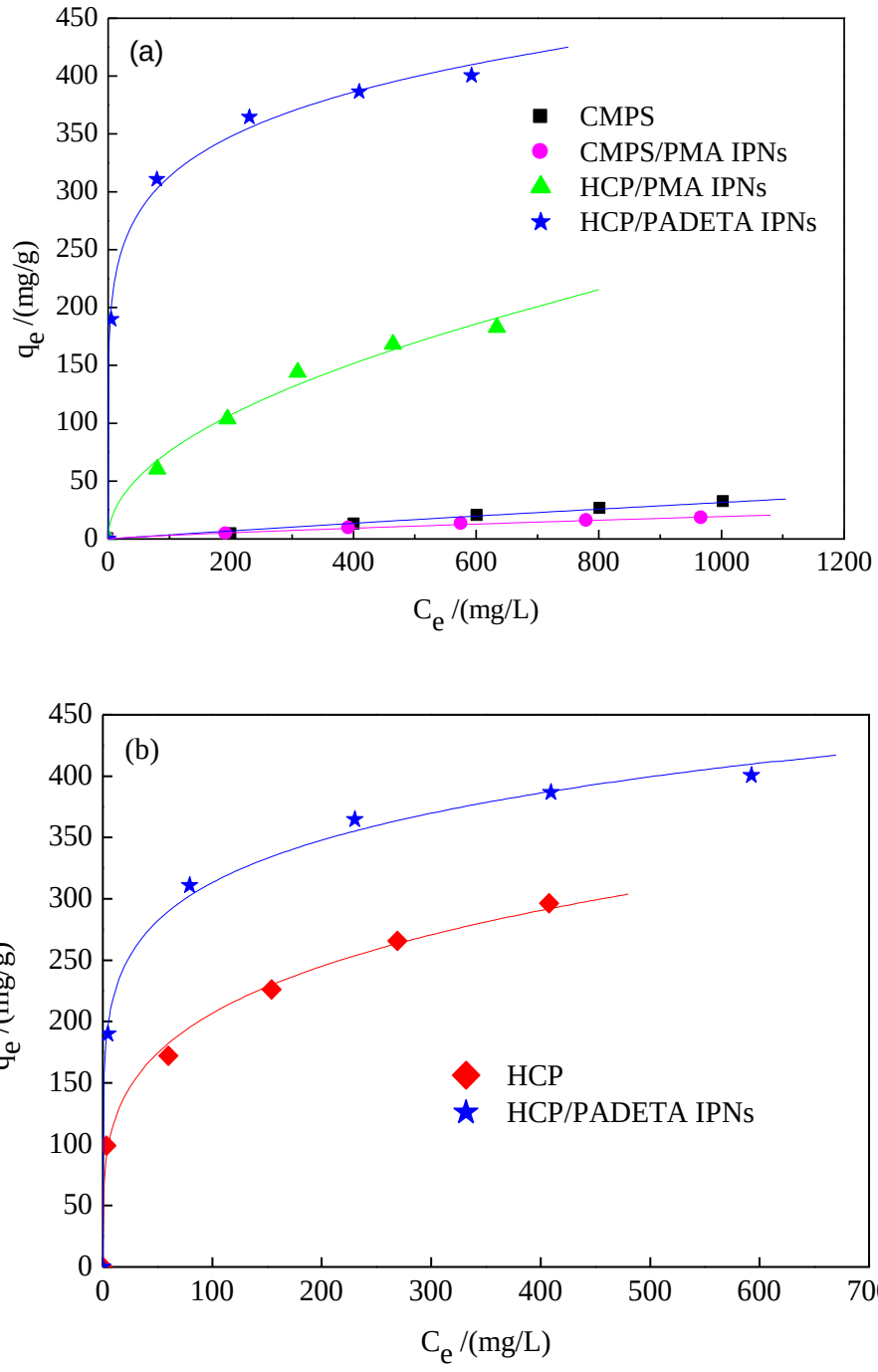

Fig. 4 Kinetic curves of salicylic acid on HCP and HCP/PADETA IPNs at 298 K.

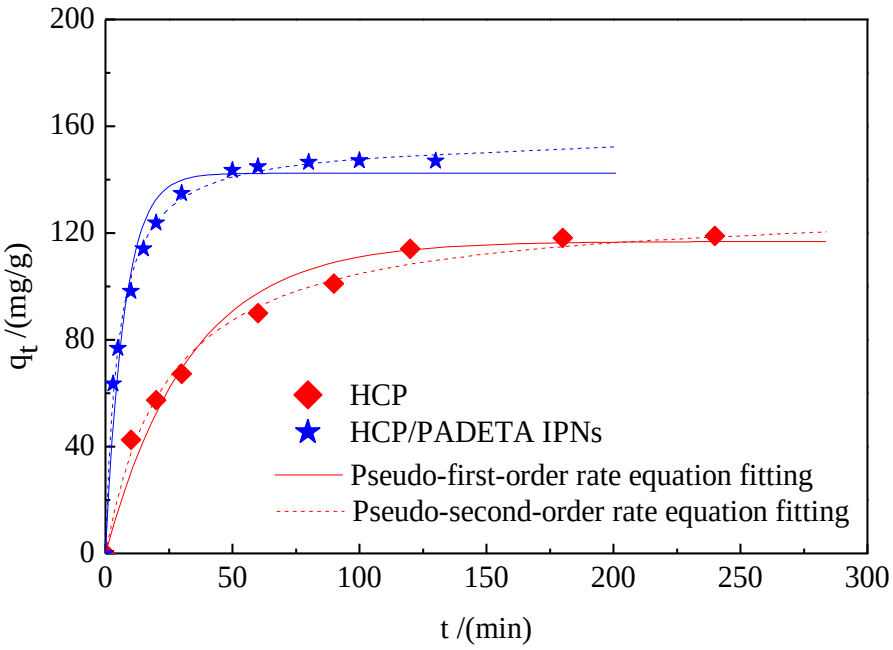

Fig. 5 Dynamic adsorption and desorption curves of salicylic acid on HCP/PADETA IPNs from aqueous solution (For the adsorption: 10.00 mL of wet resins, $C_0$=1017.3 mg/L, Flow rate=1.0 mL/min. For the desorption: 0.01 mol/L of NaOH (w/v) and 20% of ethanol (v/v) was used as the desorption solution, Flow rate=0.6 mL/min).

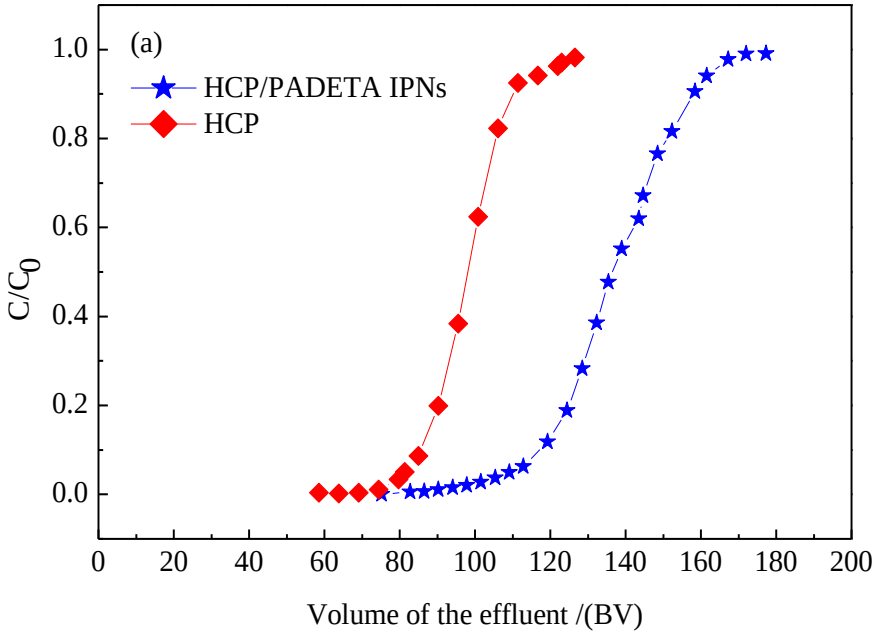


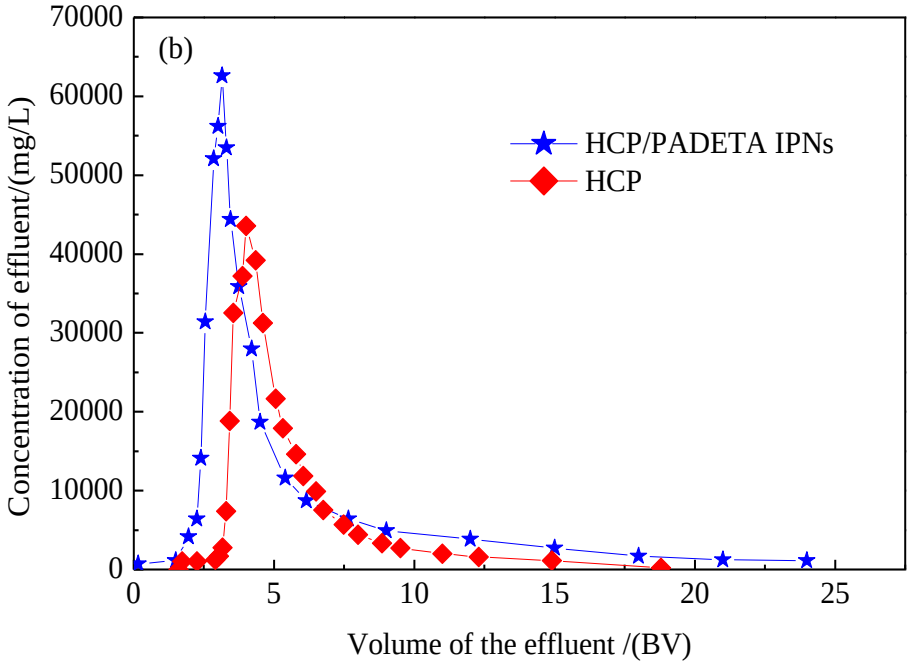

Fig. 6 Equilibrium isotherms of phenol and salicylic acid on HCP/PADETA IPNs from the single or the mixed aqueous solution at 298 K.

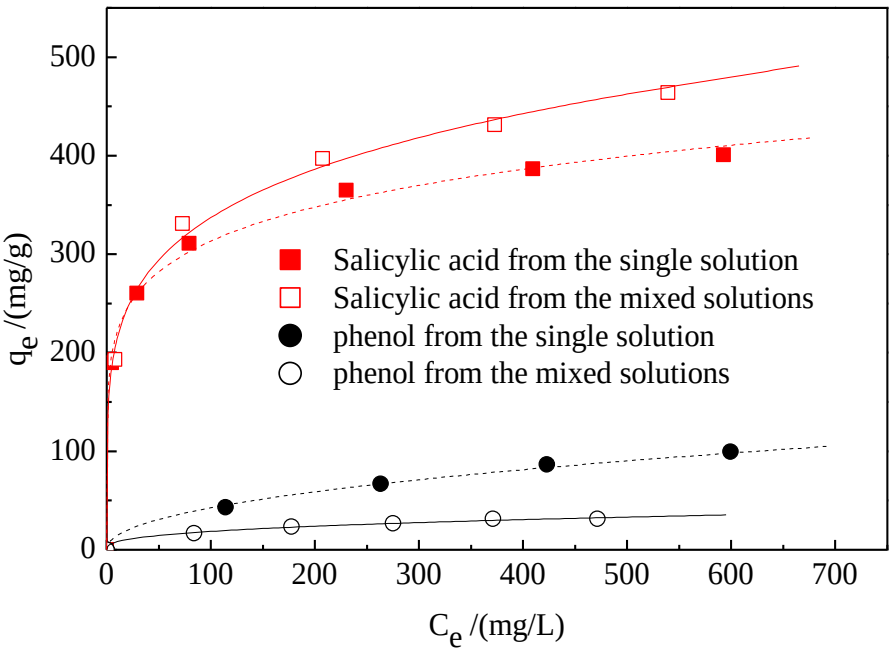

Fig. 7 Dynamic adsorption-desorption curves of phenol and salicylic acid on HCP/PADETA IPNs.

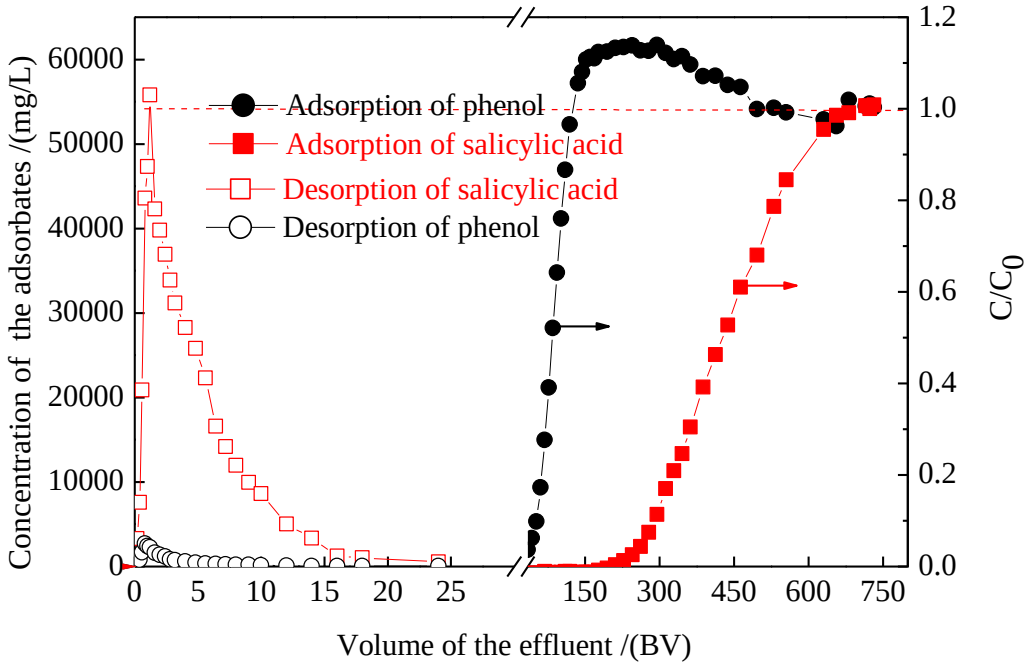

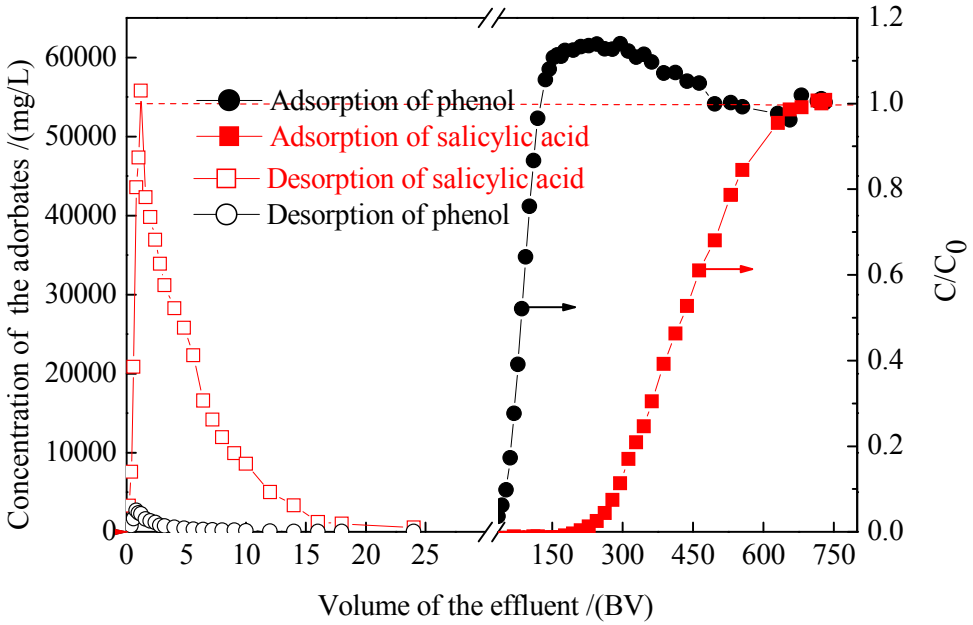


HCP/PADETA IPNs can separate salicylic acid from phenol in their mixed solution efficiently.